HARMONIC RESPONSE OF ACOUSTIC MATERIALS BY FINITE ELEMENT MODELING

JANOS LISKA[1], ANDOR MODRA[1], GABOR KONYA[1]

[1]Department of Innovative Vehicles and Materials, GAMF Faculty of Engineering and Computer Science, John von Neumann University, H-6000 Kecskemet, Izsaki St. 10., Hungary

DOI: 10.17973/MMSJ.2025_12_2025152

liska.janos@nje.hu

This study investigates the harmonic response of acoustically functional geometries fabricated via additive manufacturing, with the aim of replicating the vibrational characteristics of natural wood. Utilizing Finite Element Modelling (FEM), various complex structures were designed and analyzed to determine their dynamic behavior under harmonic excitation. The materials under investigation include Nylon12, processed through Selective Laser Sintering (SLS) as a potential substitute for traditional tonewoods in acoustic applications. Emphasis was placed on preserving critical resonance frequencies and frequency response ranges typically associated with wood-based components. The results demonstrate that tailored internal geometries can significantly influence modal behavior, offering a viable pathway toward sustainable and tunable acoustic materials. This research bridges material science and acoustic engineering by proposing an efficient modeling framework for evaluating and optimizing additively manufactured alternatives to wood.

KEYWORDS

Finite element modelling (FEM), Wood, Additive manufacturing, resonance, plastics

1 INTRODUCTION

The acoustic performance of materials plays a critical role in the design and fabrication of musical instruments, soundboards, and other audio-sensitive components. Traditionally, tonewoods such as spruce, maple, and mahogany have been the materials of choice for these applications due to their favorable mechanical and acoustic properties, including high stiffness-to-weight ratio, low internal damping, and well-defined vibrational modes [Bucur, 2006; Wegst, 2006].
These characteristics allow for efficient sound radiation, defined resonance frequencies, and tonal clarity—attributes that are essential in applications like string instruments and soundboards.

However, the increasing demand for high-quality tonewoods, coupled with environmental and economic concerns, has led to unsustainable harvesting practices, threatening both biodiversity and long-term wood availability. As a result, there is growing interest in developing alternative materials and manufacturing strategies that can replicate the desirable vibrational properties of wood while promoting sustainability [Calvano 2023].

Acoustic performance in solid materials is influenced by several intrinsic properties, including density (ρ), Young's modulus (E), and internal damping (η). A fundamental descriptor of a material's acoustic potential is the sound radiation coefficient (R), given by:

$$R = \sqrt{\frac{E}{\rho^3}} \tag{1}$$

This parameter serves as a predictor of the material's ability to radiate sound efficiently. In woods used for musical instruments, values of R are typically optimized through natural growth structures and anisotropy. The anisotropic behavior of wood—exhibiting different mechanical responses in the longitudinal, radial, and tangential directions—provides unique vibrational modes that contribute to its rich acoustic signature [Bucur, 2006].

Recent advances in Additive Manufacturing (AM) offer new opportunities to engineer internal geometries that mimic the anisotropy and frequency behavior of tonewoods. Among various AM technologies, Selective Laser Sintering (SLS) of thermoplastics like Nylon12 provides a viable route for fabricating complex, lightweight structures with high repeatability and mechanical tunability. When designed appropriately, these structures can exhibit modal behaviors analogous to those of wood, particularly in terms of harmonic response and resonance frequencies. This study applies Finite Element Modelling (FEM) as a predictive tool to investigate the dynamic behavior of engineered geometries fabricated from Nylon12 via SLS. FEM has proven effective in simulating the vibrational behavior of complex structures, including both homogeneous and composite materials [Ajoku 2006].

By incorporating material properties, boundary conditions, and harmonic excitations, FEM allows for precise modal and harmonic response analysis, critical for acoustic material design. A further benefit of FEM lies in its capacity to evaluate mode shapes and resonance peaks, which are essential for determining acoustic fidelity. For instance, the modal stiffness (k_m) and modal mass (m_m) directly influence the natural frequency of a given mode:

$$f_n = \frac{1}{2\Pi}\sqrt{\frac{k_m}{m_m}} \tag{2}$$

This relationship underlines the potential for internal geometry optimization to tailor vibrational characteristics without altering the overall mass or material composition—offering a sustainable pathway to replicate wood's acoustic profile.

Several studies have explored the replacement of wood with engineered or composite materials. [Calvano 2023] demonstrated the feasibility of using carbon fiber-reinforced polymers for violin fingerboards, while [Sinin 2024] investigated bamboo-based composites for soundboards. However, these efforts often fall short in replicating the full spectrum of acoustic behavior found in natural wood, particularly in terms of frequency response and harmonic damping.
Recent advances in Additive Manufacturing (AM) offer new opportunities to engineer internal geometries that mimic the anisotropy and frequency behavior of tonewoods. Among various AM technologies, Selective Laser Sintering (SLS) of thermoplastics like Nylon12 provides a viable route for fabricating complex, lightweight structures with high repeatability and mechanical tunability.

When designed appropriately, these structures can exhibit modal behaviors analogous to those of wood, particularly in terms of harmonic response and resonance frequencies [Zhao 2024].
This study applies Finite Element Modelling (FEM) as a predictive tóul to investigate the dynamic behavior of engineered geometries fabricated from Nylon12 via SLS. FEM has proven effective in simulating the vibrational behavior of complex structures, including both homogeneous and composite materials [Ajoku 2006; Brezas 2024]. In particular, previous works have shown that changes in geometry and material stiffness significantly influence resonance behavior, providing a strong foundation for acoustic optimization [Wang 2012; Woodward 1960; Desarnaulds 2005].

The novelty of the present study lies in its integration of AM and FEM to develop and assess acoustically functional geometries designed to emulate tonewood behavior. By leveraging internal lattice and shell-based structures, it becomes possible to fine-tune both global stiffness and localized modal response, resulting in components that preserve crucial acoustic characteristics while using recyclable, non-biological materials.

From an environmental standpoint, replacing tonewoods with functionally equivalent, 3D-printed alternatives could significantly reduce the number of trees felled for acoustic applications. This aligns with the principles of sustainable design and circular economy, emphasizing materials that can be manufactured on demand, customized for performance, and recycled at end-of-life.

In summary, this work aims to demonstrate that engineered Nylon12 components, when properly designed via FEM and fabricated through SLS, can serve as viable substitutes for wood in acoustic applications. The study contributes to a broader understanding of how material properties and geometry interact to influence vibrational behavior, with implications for sustainable material innovation in musical instrument design and other acoustic systems.

2 MATERIAL AND METHODS

2.1 *Software and Configuration*

The finite element simulations were conducted using *Ansys Workbench 2025*, while the more complex 3D modeling tasks were carried out with *PTC Creo 8.0*. For subsequent data analysis and evaluation, *Microsoft Excel* was employed to process and visualize the results.

2.2 *Configuration and Virtual Environment*

The initial investigations were performed on a square-based prism (see Figure 1), chosen for its simplicity in terms of setup and the ease with which its geometry can be evaluated analytically.

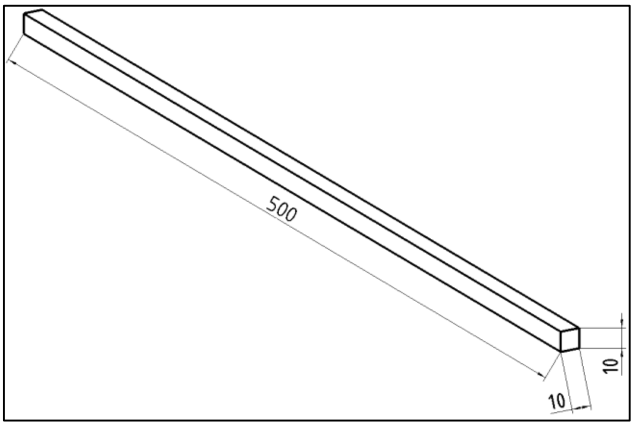

Figure 1. Examined body – Square-based prism

The simulation configuration and execution were conducted using the *Static Structural* and *Modal Analysis* modules within Ansys. To facilitate computational efficiency and to allow for a more straightforward comparison of results, parameters were created in the system.

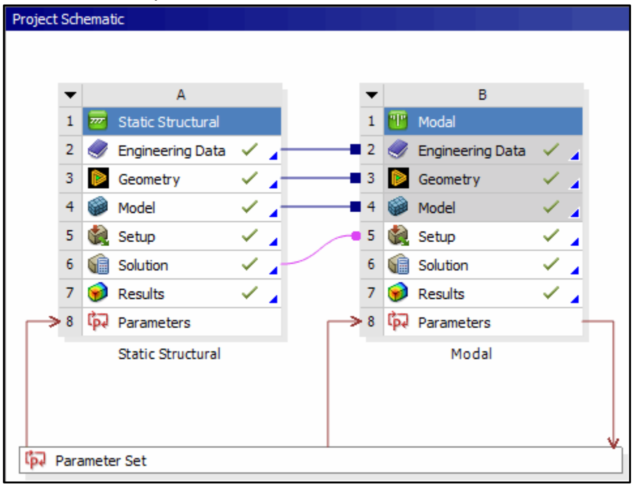

Figure 2. Project Schematic of analysis

After we prepared the body, the following constraints (Figure 3 and 4) were set.

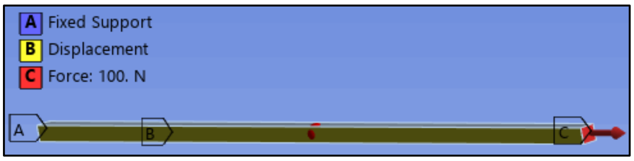

Figure 3. Constraints of body

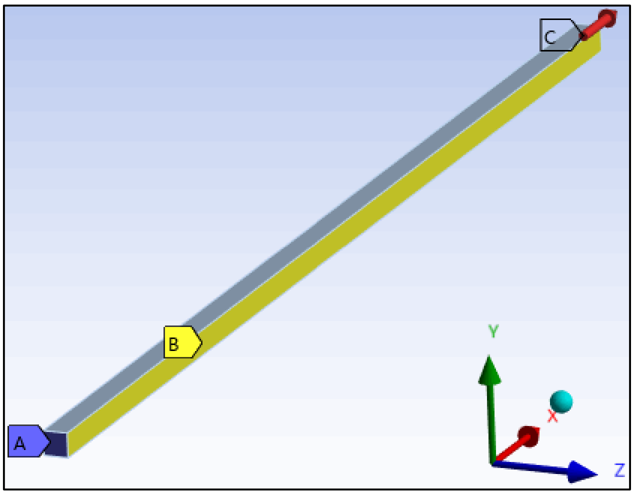

Figure 4. Constraints of body and coordinate system

The constraints depicted in the figure were applied consistently to the geometry. Constraint “A” represents a *Fixed Support*, restricting both translational and rotational motion on one end face of the prism. Constraint “B” denotes a *Displacement* boundary condition applied on a lateral face of the prism, which limits movement in the Z-direction. This ensures that the body can only move within the XY plane. This setup is essential, as our investigation focuses on a single mode of vibration, in which the nodal and reinforcement points form within a plane and no torsional deformation occurs. The end face of the prism is subjected to a 100 N axial force, labeled as constraint “C”, applied parallel to the X-axis to simulate tensile loading.

2.3 Mesh

The Mesh settings for all analyses were the following :

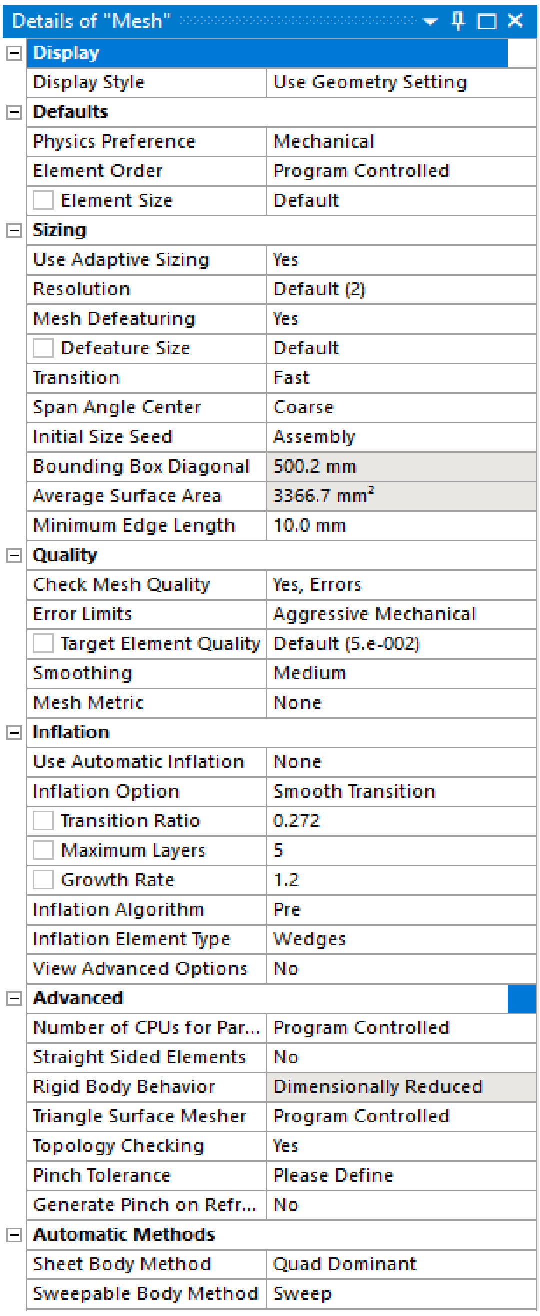

Details of "Mesh"

Display	
Display Style	Use Geometry Setting
Defaults	
Physics Preference	Mechanical
Element Order	Program Controlled
Element Size	Default
Sizing	
Use Adaptive Sizing	Yes
Resolution	Default (2)
Mesh Defeaturing	Yes
Defeature Size	Default
Transition	Fast
Span Angle Center	Coarse
Initial Size Seed	Assembly
Bounding Box Diagonal	500.2 mm
Average Surface Area	3366.7 mm²
Minimum Edge Length	10.0 mm
Quality	
Check Mesh Quality	Yes, Errors
Error Limits	Aggressive Mechanical
Target Element Quality	Default (5.e-002)
Smoothing	Medium
Mesh Metric	None
Inflation	
Use Automatic Inflation	None
Inflation Option	Smooth Transition
Transition Ratio	0.272
Maximum Layers	5
Growth Rate	1.2
Inflation Algorithm	Pre
Inflation Element Type	Wedges
View Advanced Options	No
Advanced	
Number of CPUs for Par...	Program Controlled
Straight Sided Elements	No
Rigid Body Behavior	Dimensionally Reduced
Triangle Surface Mesher	Program Controlled
Topology Checking	Yes
Pinch Tolerance	Please Define
Generate Pinch on Refr...	No
Automatic Methods	
Sheet Body Method	Quad Dominant
Sweepable Body Method	Sweep

Figure 5. Meshing of the body

2.4 Parametric Materials

Among the simulation settings, the material properties were defined as variable parameters (Table 1.) within the parametric framework. Three primary material characteristics were studied: *Density*, *Young’s Modulus*, and *Poisson’s Ratio*. For each property, 10 distinct material variants were generated, differing solely in the selected property. For example, the first set of 10 materials varied only in density, the second set in Poisson’s ratio, and so forth.

Variables	Value	Unit of Measure
00Density	500	kg/m^3
01Density	600	kg/m^3
02Density	700	kg/m^3
03Density	800	kg/m^3
04Density	900	kg/m^3
05Density	1000	kg/m^3
06Density	1100	kg/m^3
07Density	1200	kg/m^3
08Density	1300	kg/m^3
09Density	1400	kg/m^3
00Young-Modulus	1000	Mpa
01Young-Modulus	2000	Mpa
02Young-Modulus	3000	Mpa
03Young-Modulus	4000	Mpa
04Young-Modulus	5000	Mpa
05Young-Modulus	6000	Mpa
06Young-Modulus	7000	Mpa
07Young-Modulus	8000	Mpa
08Young-Modulus	9000	Mpa
09Young-Modulus	10000	Mpa
00Poisson	0.3	-
01Poisson	0.31	-
02Poisson	0.32	-
03Poisson	0.33	-
04Poisson	0.34	-
05Poisson	0.35	-
06Poisson	0.36	-
07Poisson	0.37	-
08Poisson	0.38	-
09Poisson	0.39	-

Table 1. Table of parameterised material properties

Modal analyses were performed for each material, where geometries remained identical, but material qualities differed. As a theoretically infinite number of standing wave modes can occur in a solid body, only the *first mode* was examined, since higher-order harmonics increase proportionally regardless of material or geometry. Considering the boundary conditions, we specifically studied the first vibration mode of a cantilevered structure, where the length of the body corresponds to one-quarter of the standing wave:

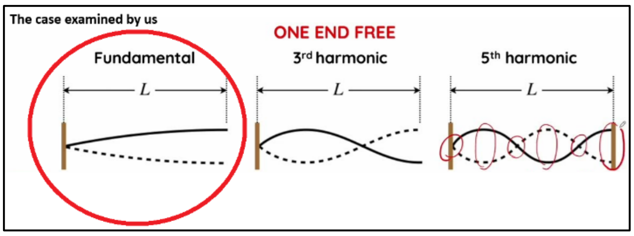

Figure 6. Standing wave on a one-fixed-end body.

2.5 *Real Materials*

We also created materials based on real wood and plastics properties, so that we could compare engineering tonewood and plastic materials. The material properties are listed in the following table :

Material	Density (ρ) [kg/m³]	Young-modulus (E) [MPa]	Poisson's ratio (ν)	Hardness (Janka) [lbf]	P1 – Stiffness Coefficient
Nylon 12	1010	1850	0.39	1600	1.20E-05
Rosewood	850	12000	0.3	2500	1.00E-04
Maple	650	9500	0.35	1450	7.00E-05
Ebony	1050	16000	0.3	3200	1.20E-04
Mahogany	550	8500	0.36	900	7.50E-05
Spruce	450	11000	0.37	380	3.00E-05

Table 3. Table of engineering material properties [Ross 2010], [Wegst 2006]

3 RESULTS OF MODAL ANALYSIS

3.1 *Behavior of parametric materials*

The behavior of virtual parameterised materials and the own frequency of the body can be seen in Fig. 6-8 below.

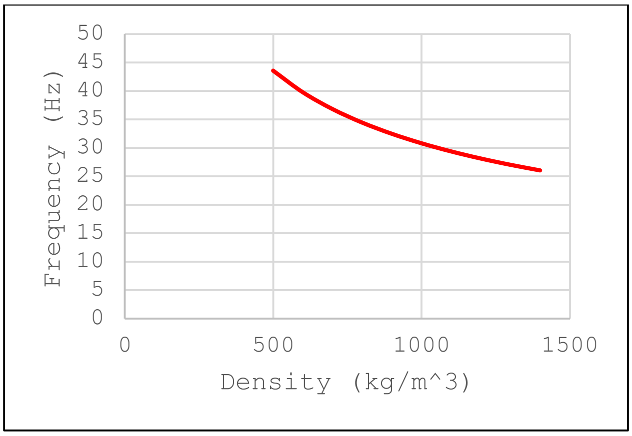

Figure 7. Frequency vs Density

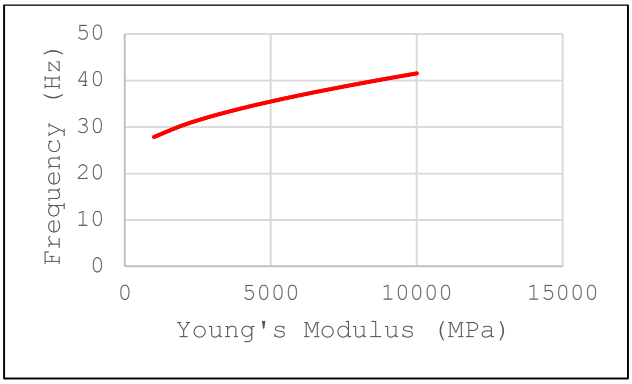

Figure 8. Frequency vs Young's Modulus

The stiffness coefficient denotes the modal stiffness of the structure for a given vibration mode, incorporating both the material's elastic properties and the geometry's mode shape, and—together with modal mass—determining the natural frequency [Ajoku 2006; Bucur, 2006; Wegst, 2006].

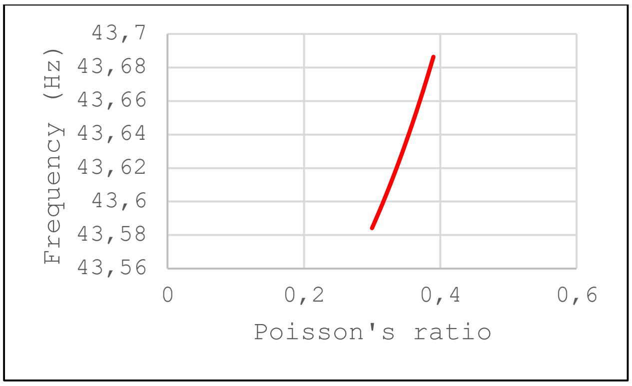

Figure 9. Frequency vs Poisson's Ratio

From the resulting curves, correlations between material properties and the natural frequency of the structure can be inferred.

This analysis was extended to six additional materials, which will be discussed in subsequent sections. Based on the evaluated parameters (as presented in Table 3.), natural frequencies specific to each material were obtained. In these cases, multiple material parameters varied simultaneously.

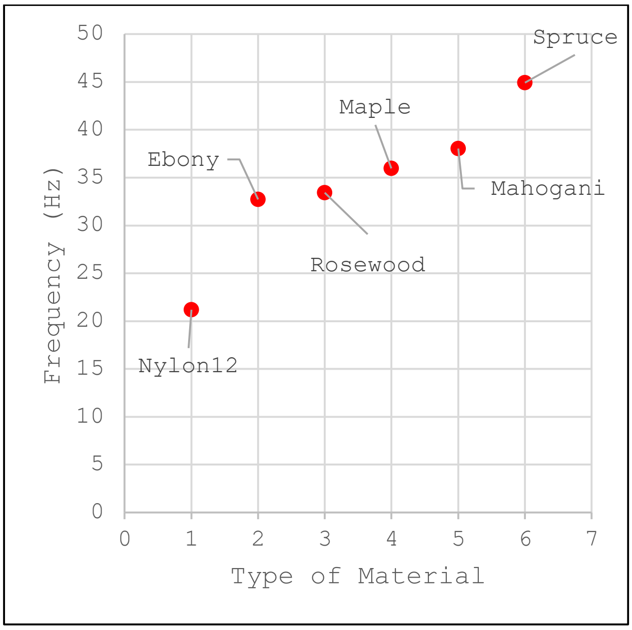

Figure 10. Frequency vs Materials of **Table 3.**

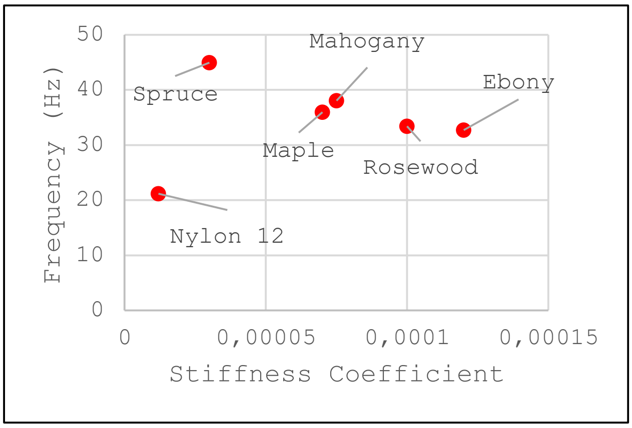

Figure 11. Frequency vs Material Stiffness

It was observed, for instance, that the structure made from *Nylon 12* exhibited a lower natural frequency compared to those constructed from various wood types. Since all tested structures shared identical geometries and boundary conditions, the variation in natural frequency must be attributed to differences in wave propagation speed across the materials. The precise relationships among these variables will be the subject of future investigation.

4 MEASUREMENT OF MATERIAL DAMPING

4.1 Configuration and Virtual Environment

In the following phase of experimentation, the damping characteristics of the materials will be analyzed. The Ansys software suite was configured with the following solvers:

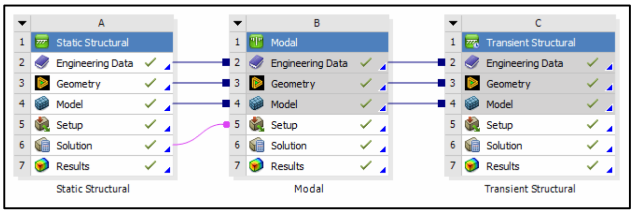

Figure 12. Project Schematic for Damping measurement

Within the *Geometry* tab, the same structure was recreated. In the *Model* tab, identical boundary conditions were applied across all three solvers (*Static Structural*, *Modal*, and *Transient Structural*), as illustrated by the project interlinking (see Fig. 11). An additional constraint was introduced exclusively in the *Transient Structural* module, a displacement condition which was essential to initiate oscillation in the structure (see Fig 13).

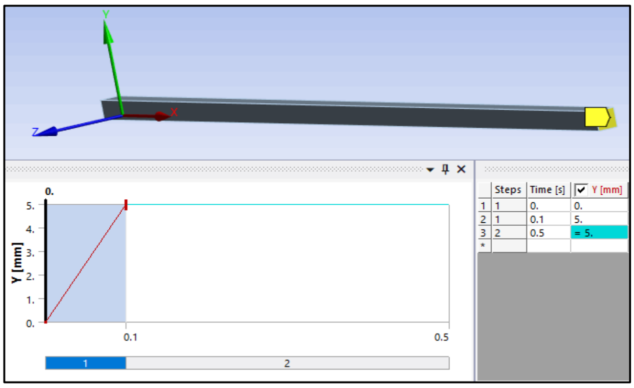

Figure 13. Displacement with Time Steps

This Displacement constraint induced a 5 mm deflection along the Y-axis, as specified in the tabulated input data, and was released at t = 0.1 s. The sudden release initiated a free vibration in the deformed structure, leading to an oscillatory motion. The following settings were configured in the analysis:

Details of "Solution Information"

Solution Information	
Solution Output	Force Convergence
Newton-Raphson Residuals	0
Identify Element Violations	0
Update Interval	2.5 s
Display Points	All
FE Connection Visibility	
Activate Visibility	Yes
Display	All FE Connectors
Draw Connections Attached To	All Nodes
Line Color	Connection Type
Visible on Results	No
Line Thickness	Single
Display Type	Lines

Figure 14. Settings in Transient Solution Tab

A *Deformation Probe* was placed at the vertex on the free end of the structure (see Fig. 15.) to track the displacement of that specific point over time:

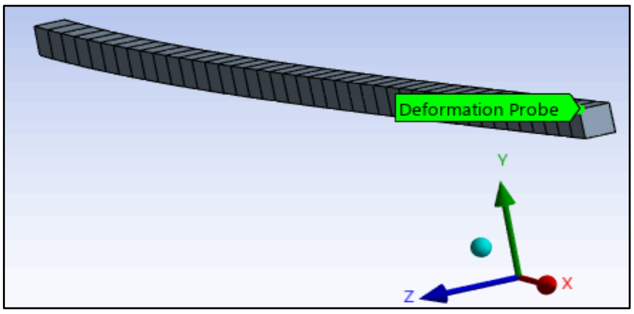

Figure 15. Placement of Deformation probe

The output data was exported from the *Tabular Data* view, and for each material, the displacement-time curves were plotted in Microsoft Excel.

5 RESULTS OF MATERIAL DAMPING

In the following the results of Material damping can be seen. The simulation processed the first 2 seconds of the oscillation.

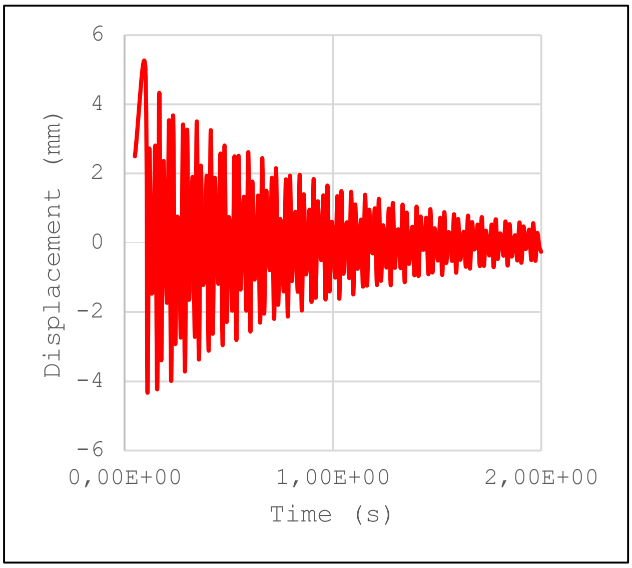

Figure 16. Damping of Spruce over Time

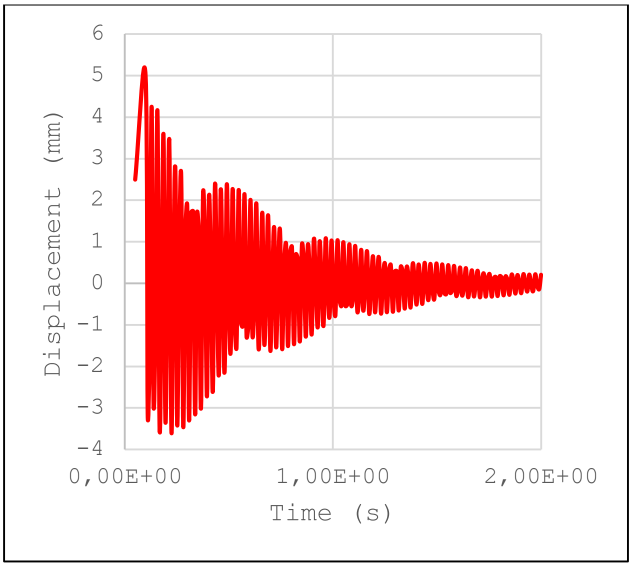

Figure 17. Damping of Maple over Time

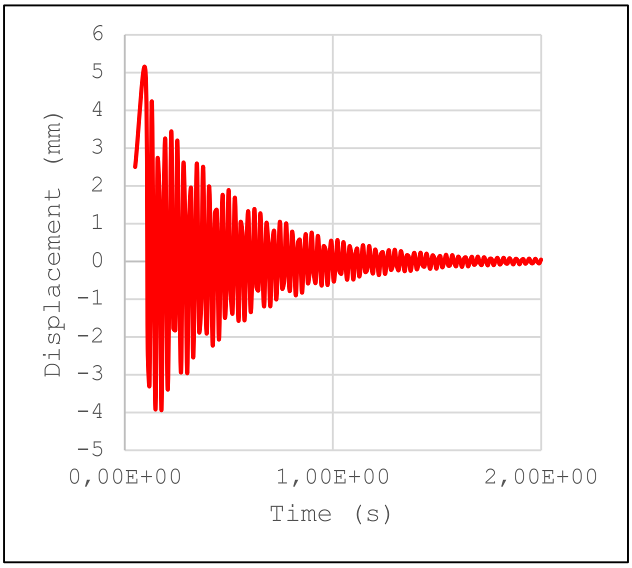

Figure 18. Damping of Ebony over Time

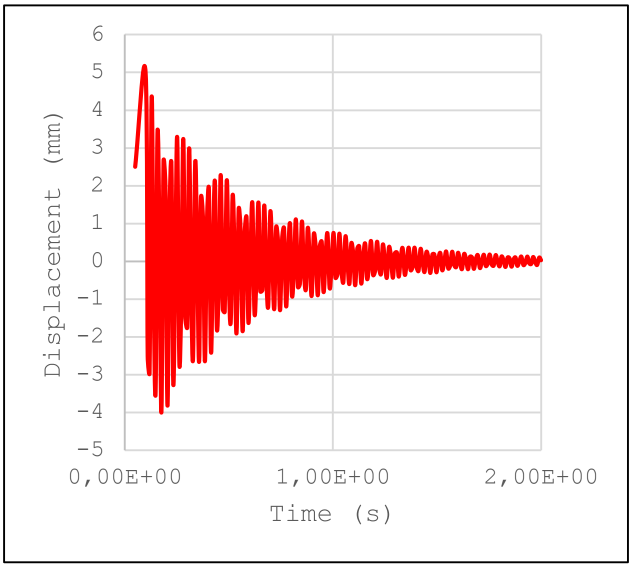

Figure 19. Damping of Rosewood over Time

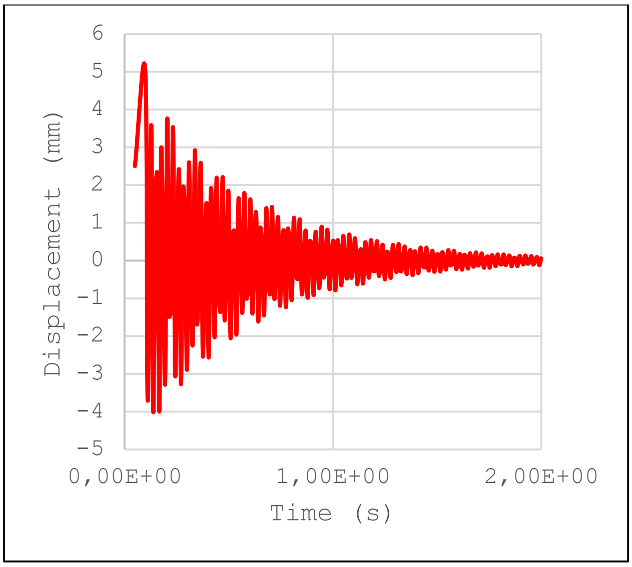

Figure 20. Damping of Mahogany over Time

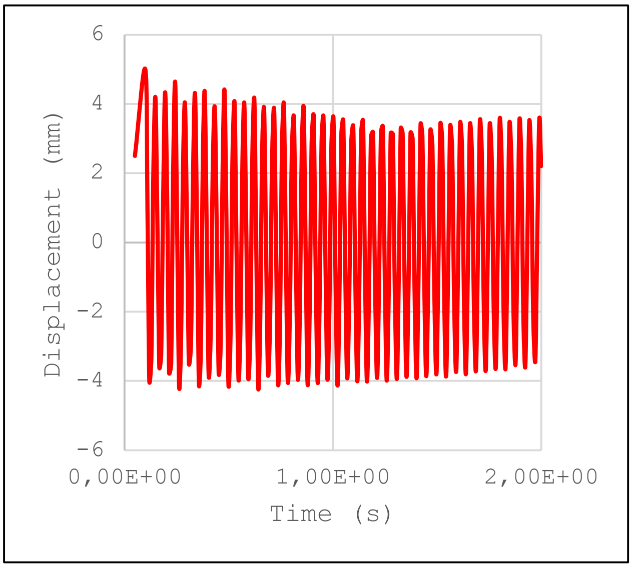

Figure 21. Damping of Nylon 12 over Time

In the case of Nylon 12, the measurement was repeated on a structure of identical external dimensions but with an internally lightened design, yet increasing its damping capacity. The damping simulations provided insight into the vibrational decay characteristics of each tested material. For natural woods such as spruce and maple, oscillation amplitudes decreased gradually, retaining over 60% of their initial displacement after 0,5 seconds, indicating high damping behavior. In contrast, Nylon 12 exhibited a lower decay, with displacement dropping only by 15% within the same timeframe. When an internally structured version of Nylon 12 was used, the damping curve changed significantly—showing a faster decay rate compared to the solid version (see Fig. 21 and 22). Immediately after release, the nylon 12 rod exhibited a rapid loss of its initial 5 mm displacement. By the time it reached the opposite side, the oscillation amplitude had diminished to just 3 mm, followed by a further pronounced decay. This clearly proves, that internal geometry can be used as an effective design parameter to control damping performance. These results confirm the sensitivity of dynamic response not only to material composition but also to internal structure.

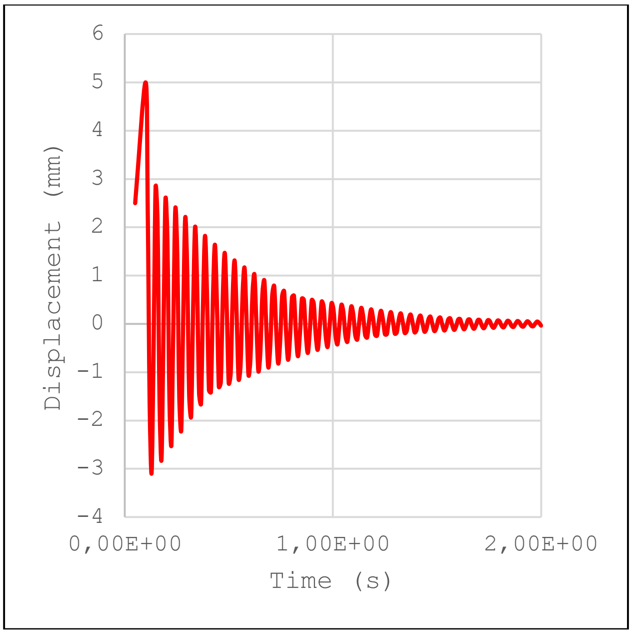

Figure 22. Damping in Internally Structured body of Nylon 12 over Time

6 MEASUREMENT OF HARMONIC RESPONSE

6.1 *Configuration and virtual environment*

In this phase, we examined the body's harmonic response as a function of the material type and internal structure. The Ansys software suite was configured with the following solvers:

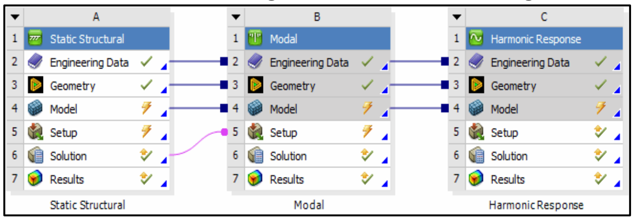

Figure 23. Project Schematic for Harmonic Response measurement

The project interlinking provided identical boundary conditions in all three solvers above. An additional constraint was introduced exclusively in the *Harmonic Response* module, a Force condition which was essential to apply frequency sweep on the body (see Fig. 24 and 25).

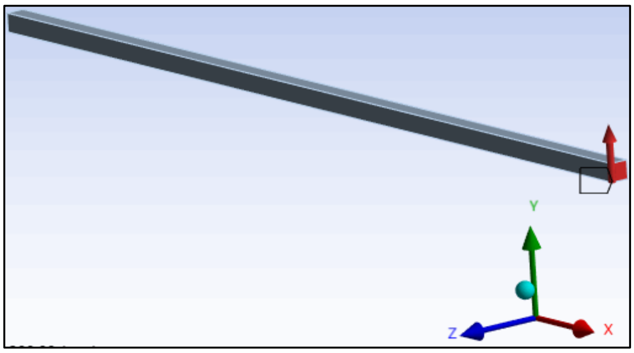

Figure 24. Placement of Force applied in frequency sweep

The Analysis settings in Harmonic Response were the following :

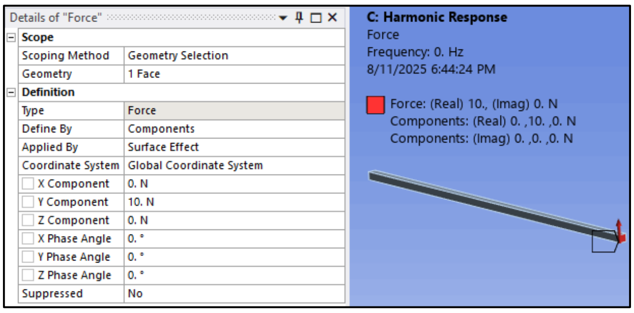

Scope	
Scoping Method	Geometry Selection
Geometry	1 Face
Definition	
Type	Force
Define By	Components
Applied By	Surface Effect
Coordinate System	Global Coordinate System
X Component	0. N
Y Component	10. N
Z Component	0. N
X Phase Angle	0. °
Y Phase Angle	0. °
Z Phase Angle	0. °
Suppressed	No

Figure 25. Properties of Force applied

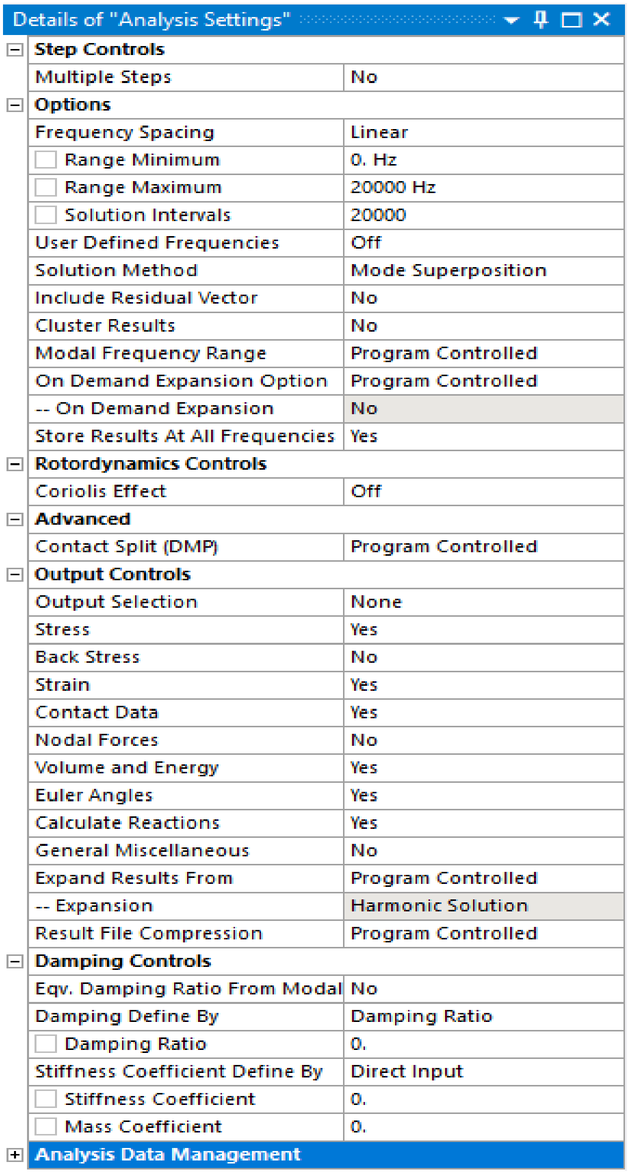

Details of "Analysis Settings"

Step Controls	
Multiple Steps	No
Options	
Frequency Spacing	Linear
Range Minimum	0. Hz
Range Maximum	20000 Hz
Solution Intervals	20000
User Defined Frequencies	Off
Solution Method	Mode Superposition
Include Residual Vector	No
Cluster Results	No
Modal Frequency Range	Program Controlled
On Demand Expansion Option	Program Controlled
-- On Demand Expansion	No
Store Results At All Frequencies	Yes
Rotordynamics Controls	
Coriolis Effect	Off
Advanced	
Contact Split (DMP)	Program Controlled
Output Controls	
Output Selection	None
Stress	Yes
Back Stress	No
Strain	Yes
Contact Data	Yes
Nodal Forces	No
Volume and Energy	Yes
Euler Angles	Yes
Calculate Reactions	Yes
General Miscellaneous	No
Expand Results From	Program Controlled
-- Expansion	Harmonic Solution
Result File Compression	Program Controlled
Damping Controls	
Eqv. Damping Ratio From Modal	No
Damping Define By	Damping Ratio
Damping Ratio	0.
Stiffness Coefficient Define By	Direct Input
Stiffness Coefficient	0.
Mass Coefficient	0.
Analysis Data Management	

Figure 26. Analysis settings in Harmonic Response

The frequency sweep analysis was applied on the 6 materials (see Table 3). In the case of Nylon 12, the analysis was repeated using the internally structured body.

7 RESULTS OF HARMONIC RESPONSE ANALYSIS

In the following the results of Harmonic Response can be seen:

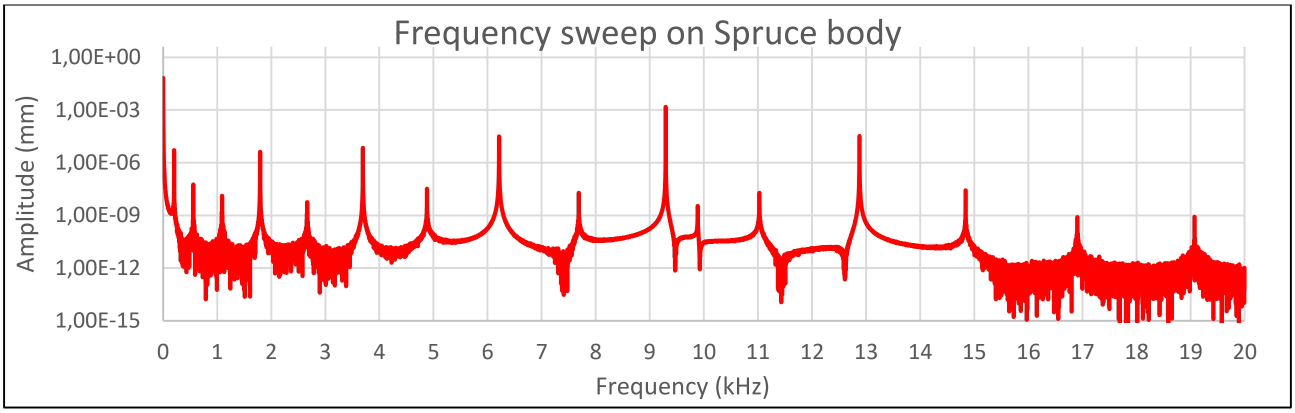

Figure 27. Frequency sweep on Spruce body

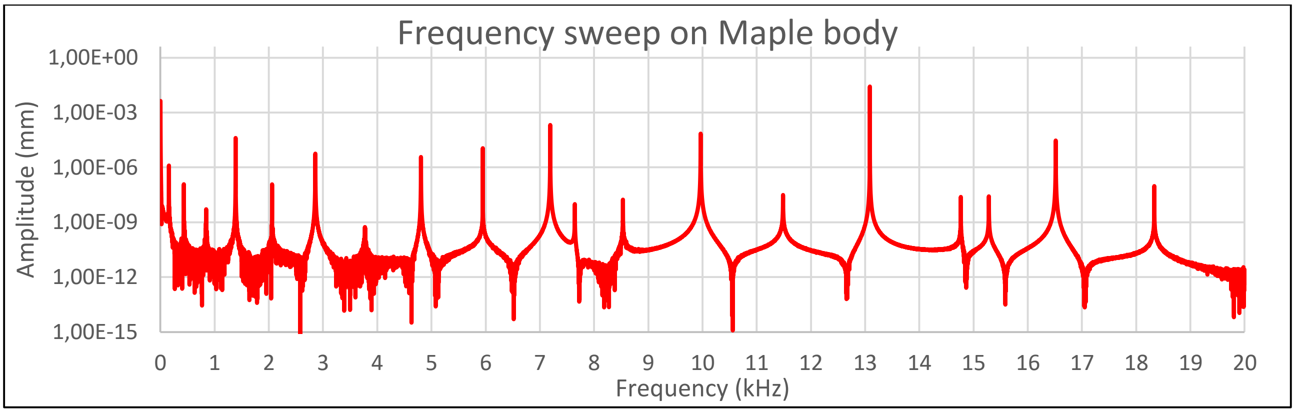

Figure 28. Frequency sweep on Maple body

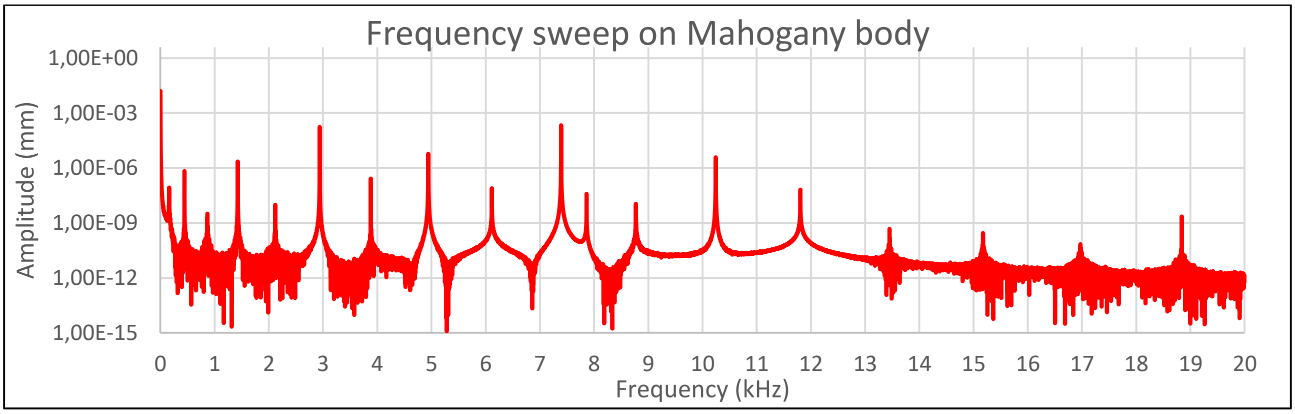

Figure 29. Frequency sweep on Mahogany body

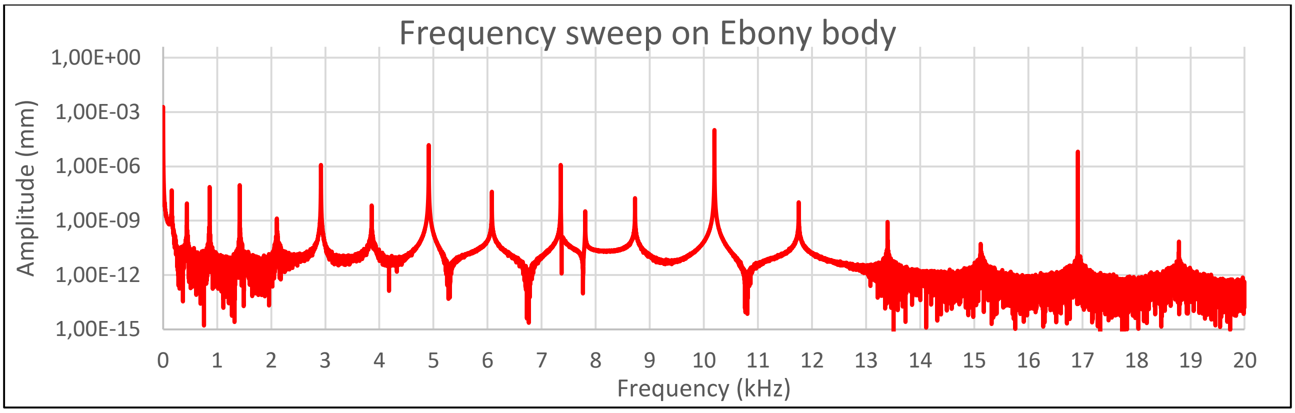

Figure 30. Frequency sweep on Ebony body

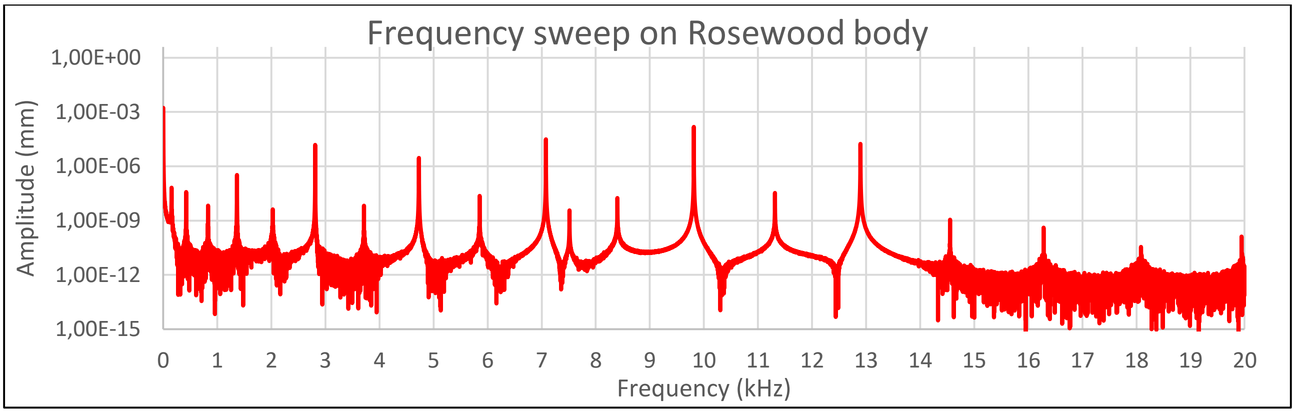

Figure 31. Frequency sweep on Rosewood body

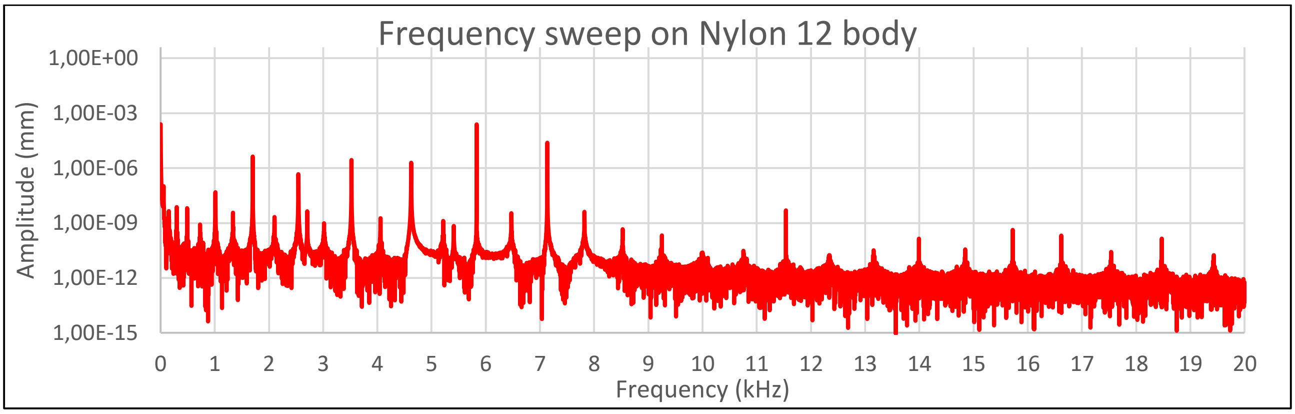

Figure 32. Frequency sweep on Nylon 12 body

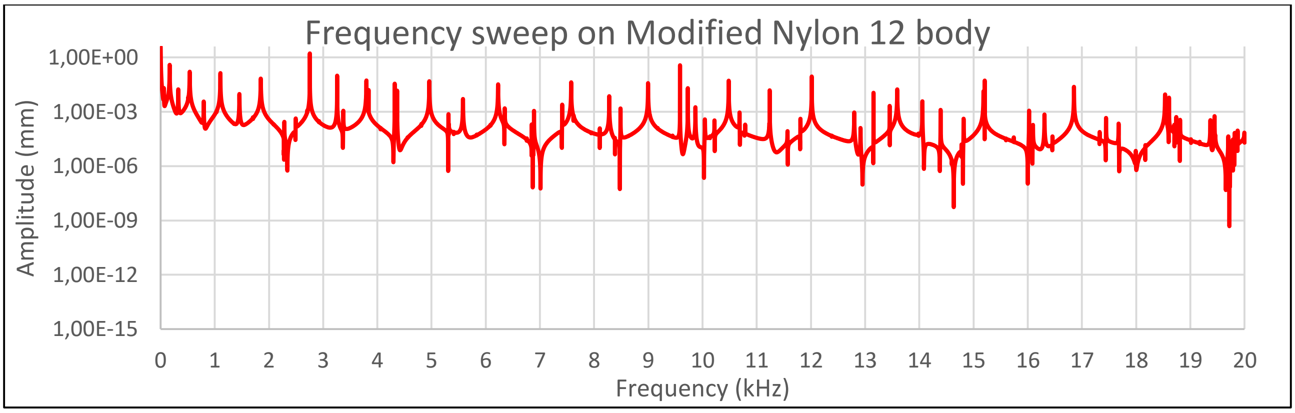

Figure 33. Frequency sweep on Modified Nylon 12 body

The diagrams show, that different materials have amplitude peaks at different places. When a structure is subjected to a forced vibration at a specific frequency, it can respond in different ways. In some cases, the excitation frequency coincides with one of the structure's natural frequencies, causing it to resonate—amplitude increases occur at these points. At the opposite extreme, if the excitation frequency is far from any of the natural frequencies, the imposed vibration is largely suppressed, and the oscillations are effectively canceled. A comparable example is when attempting to push a swing at a certain speed and period: if the input frequency does not match the swing's natural frequency, the motion cannot be sustained; conversely, even a small force applied at the correct frequency can result in a significant increase in swing amplitude. Thus, a structure can respond to forced vibration with a large amplitude—producing a positive peak—or it can attenuate the vibration at that point—producing a negative peak. When a guitar string is plucked, multiple frequencies and harmonics are present in its vibration. Because the string is coupled to the guitar body, the body absorbs certain frequencies while amplifying others, thereby shaping a unique tonal spectrum. Figures 27–31 clearly show that the amplitudes of the different wood types vary. It can be stated that maple, rosewood, and ebony exhibit greater vibrations primarily in the higher and mid-frequency ranges, while in other ranges they tend to have a damping effect. Mahogany, another widely used tonewood, displayed higher vibrations mainly in the lower-mid frequency range. Based on these characteristics, luthiers often combine different wood types in order to achieve the tonal spectrum envisioned by the designers. These properties cannot be classified as inherently "good" or "bad"; rather, they indicate which instrument construction they are most suitable for (e.g., maple is typically associated with Telecasters, while mahogany is more common in Gibsons).

Our research also demonstrates, as seen in Figure 32, that Nylon-12 is generally unsuitable as a tonewood due to its predominantly damping effect. However, through geometric modifications, it is possible to make it behave more similarly (Figure 33) to the aforementioned wood types.

8 CONCLUSIONS

The conducted simulations and analyses confirm that Nylon 12, a widely available additive-manufactured plastic, displays significantly different acoustic properties compared to traditional tonewoods. Specifically, the modal analysis (see Figures 7-11) showed that the first natural frequency of Nylon 12 (approx. 21 Hz) was substantially lower than that of spruce (45 Hz), maple (36 Hz), and mahogany (38 Hz). This indicates a 40–50% reduction in vibrational frequency, which can be attributed to the lower Young's Modulus of Nylon 12, measured at approximately 1,85 GPa, compared to 9–16 GPa for woods.

In terms of material damping (see Figures 16-22), Nylon 12 demonstrated a faster amplitude decay, with the oscillation magnitude reduced only to 70% of its initial value within the first 2 seconds, whereas spruce and maple lost above 90% amplitude in the same time frame. However, introducing an internally structured, lightweight design in the Nylon 12 sample improved its damping behavior approximately to the level of wood damping measures, allowing it to mimic the acoustic stiffness of woods while maintaining similar stiffness-to-weight ratios. The parametric studies further reinforced the sensitivity of natural frequency to material stiffness. A tenfold increase in Young's Modulus—from 1 GPa to 10 GPa—resulted in a nearly 50% increase in natural frequency, highlighting the dominant role of stiffness in harmonic response. A threefold increase in Density variations led to a frequency drop by 44%, while Poisson's ratio had a barely noticable impact across the tested range (0,30–0,39).

Harmonic response analyses show that each material has its own characteristic frequency behavior, with certain frequencies being absorbed and others amplified. For Nylon 12, much of the frequency range exhibits a muted response—low amplitudes at higher frequencies and a stronger presence of lower tones. The modified Nylon 12, on the other hand, produces a much cleaner spectrum. The modified Nylon 12, on the other hand, produces a much cleaner spectrum, and although its overall response remains relatively flat, distinct peaks appear that can be tuned through modeling to specific target values, reproducing the vibrational characteristics commonly found in wood-based materials.

Taken together, the results indicate that by adjusting internal geometries and exploiting the parametric design freedom of additive manufacturing, Nylon 12 structures can be tuned to mimic up to 60–70% of the frequency behavior of natural tonewoods (on the base of the harmonic response results in the modified Nylon12 body). It is important to note, that we analyzed only one 3D printable material the Nylon 12. In the future involving the composit version of Nylon 12 (Nylon 12 CF) in our study, with additive manufacturing we can create geometries, that mimic the acoustic properties of tonewoods at a very high level.

This study supports the potential for developing customized, sustainable acoustic components, especially in the context of musical instrument making and sound-sensitive product design.

REFERENCES

[Bucur 2006] Bucur, V. Acoustics of Wood, 2nd Edition, The Journal of the Acoustical Society of America, AIP Publishing, 2006, Vol.119, No.6, 3506. https://doi.org/10.1121/1.2197787.

[Wang 2012] Wang, Z., Li, L., Gong, M., Measurement of dynamic modulus of elasticity and damping ratio of wood-based composites using the cantilever beam vibration technique, Construction and Building Materials, 2012, Vol.28, No.1, pp. 831-834. https://doi.org/10.1016/j.conbuildmat.2011.09.00.

[Wegst 2006] Wegst, U.G.K. Wood for Sound, American Journal of Botany, 2006, Vol.93, No.10, pp. 1439–1448. https://doi.org/10.3732/ajb.93.10.1439.

[Zhao 2024] Zhao, B., et al. A nonlinear damped metamaterial: Wideband attenuation with nonlinear bandgap and modal dissipation, Mechanical Systems and Signal Processing, 2024, Vol.208, 111079 https://doi.org/10.1016/j.ymssp.2023.111079.

[Brezas 2024] Brezas. S, et al. Review of Manufacturing Processes and Vibro-Acoustic Assessments of Composite and Alternative Materials for Musical Instruments. Applied Sciences, 2024, Vol.14, No.6, 22293. https://doi.org/10.3390/app14062293.

[Woodward 1960] Woodward, A.E., Crissman, J.M., & Sauer, J.A. Investigations of the dynamic mechanical properties of some polyamides, Journal of Polymer Science, 1960, Vol.44, No.143, pp 23-34. https://doi.org/10.1002/pol.1960.1204414303.

[Calvano 2023] Calvano, S., et al. Use and sustainability of wood in acoustic guitars: An overview based on the global market, Heliyon, 2023, Vol.9, No.4: e15218 https://doi.org/10.1016/j.heliyon.2023.e15218.

[Sinin 2024] Sinin, A.S., et al. Acoustic characteristics of bamboo-based guitar – A case study. Bioresources, 2024, Vol.20, No.1, pp 140-154. https://doi.org/10.15376/biores.20.1.140-154.

[Ajoku 2006] Ajoku, U., Hopkinson. N., & Caine, M. Experimental measurement and finite element modelling of the compressive properties of laser sintered Nylon-12, Materials Science and Engineering: A, 2006, Vol.428, No.1-2, pp 211-216. https://doi.org/10.1016/j.msea.2006.05.019.

[Desarnaulds 2005] Desarnaulds, V., et al. Sustainability of acoustic materials and acoustic characterization of sustainable materials, Proceedings of the 12th international congress on sound and vibration, 2005, pp 1-8

[Formlabs 2022a] Formlabs. Nylon 12 Technical Data Sheet [online]. 2022 [cited 2025-05-10]. Available from https://media.formlabs.com/m/2a02034348060e54/original/-ENUS-Nylon-12-TDS.pdf.

[Formlabs 2022b] Formlabs. Nylon 12 Tough Technical Data Sheet [online]. 2022 [cited 2025-05-10]. Available from https://media.formlabs.com/m/193cb61bc0ace02b/original/-ENUS-Nylon-12-Tough-TDS.pdf.

[Ross 2010] Ross, R.J., Wood Handbook: Wood as an Engineering Material, USDA Forest Service, Forest Products, General Technical Report FPL-GTR-190, 2010, pp 1-509. https://doi.org/10.2737/FPL-GTR-190.

[DesignerData 2025] DesignerData. Polyamide 12 [online]. 2025 [cited 2025-05-10]. Available from https://designerdata.nl/materials/plastics/thermo-plastics/polyamide-12.

CONTACTS:

Janos Liska, PhD., **associate professor**
Department of Innovative Vehicles and Materials, GAMF Faculty of Engineering and Computer Science, John von Neumnann University
Izsaki St. 10., Kecskemet, 6000, Hungary
liska.janos@nje.hu